

doi: 10.15407/ujpe60.09.0917

V.M. SKLYARCHUK,<sup>1</sup> YU.O. PLEVACHUK,<sup>1</sup> A.O. OMELCHUK,<sup>2</sup> N.V. FAIDYUK<sup>2</sup><sup>1</sup> Ivan Franko National University of Lviv

(8, Kyrylo i Mefodiy Str., Lviv 79005, Ukraine; e-mail: plevachuk@mail.lviv.ua)

<sup>2</sup> Vernadskyi Institute of General and Inorganic Chemistry, Nat. Acad. of Sci. of Ukraine

(32/34, Academician Palladin Ave., Kyiv 03680, Ukraine)

## VISCOSITY, CONDUCTIVITY, AND THERMOELECTRIC POWER IN IONIC AND ION-ELECTRON EUTECTIC LIQUID SYSTEMS

PACS 71.22.+i, 72.15.Eb

*The temperature dependences of viscosity, conductivity, and thermoelectric power in ionic and ion-electron liquid systems with eutectic and near-eutectic compositions have been studied and compared in a wide temperature interval, which includes the melting temperatures of the examined alloys.*

*Key words:* ionic liquid systems, ion-electron liquid systems, eutectic, viscosity, conductivity, thermoelectric power.

### 1. Introduction

In accordance with the classification [1,2], liquid metals and semiconductors, which were started to be widely used, in due course, in the power engineering, are called ion-electron liquids, because it is the behavior of ionic and electronic subsystems that governs their basic properties. Such liquids belong to disordered media, which find the more and more wide application in the engineering and modern technologies, e.g., in the development of fourth-generation atomic reactors. The modern nuclear power engineering of a new generation, which is intended to eliminate the radioactive environmental contamination and the propagation of the technology aimed at producing weapons-grade isotopes, assumes the development of fourth-generation reactors of six types, with a proper place among them being occupied by transmutation reactors. The latter are created in order to completely burn out weapons isotopes and to destroy radioactive waste taking advantage of the accelerator-driven transmutation of long-term radionuclides [3].

Suitable media for the implementation of such a transmutation are molten salt fuel mixtures, which gave a name to one of the types of fourth-generation reactors, molten salt reactors [4]. As nuclear fuel carriers, the mixtures of metal fluorides are recommended to be used, which have insignificant total

thermal neutron capture cross-sections. This work was aimed at comparing the physical properties – namely, viscosity, electric conductivity, and thermal emf – of ionic (salt melts) and ion-electron (metal melts) eutectic fluid systems as probable heat carriers in power installations.

### 2. Experimental Part

The viscosity measurements were carried out on a computer-assisted viscometer with a rotating crucible [5]. Measurement cells were fabricated from graphite in the form of cylindrical containers with an internal diameter of 14 mm and 30 mm in height. The period and the logarithmic decrement of oscillation damping were determined, by using an optical system. The viscosity was calculated using a modified Roscoe equation for cylindrical specimens with open surface. Measurements were carried out in an atmosphere of 90%Ar + 10%H<sub>2</sub>. A uniform temperature field was maintained with an accuracy of 5 K in a chamber in the interval up to 800 K. The temperature was measured with the help of a WRe-5/20 thermocouple located under the container. The error of viscosity measurements did not exceed 3%.

The measurements of the conductivity and the thermal emf were carried out in the argon atmosphere with a pressure up to 10 MPa, by using the 4-point contact method. Measurement cells fabricated from pressed boron nitride in the form of vertical containers 60 mm in height and 3 mm in diameter

© V.M. SKLYARCHUK, YU.O. PLEVACHUK,  
A.O. OMELCHUK, N.V. FAIDYUK, 2015

ISSN 2071-0186. Ukr. J. Phys. 2015. Vol. 60, No. 9

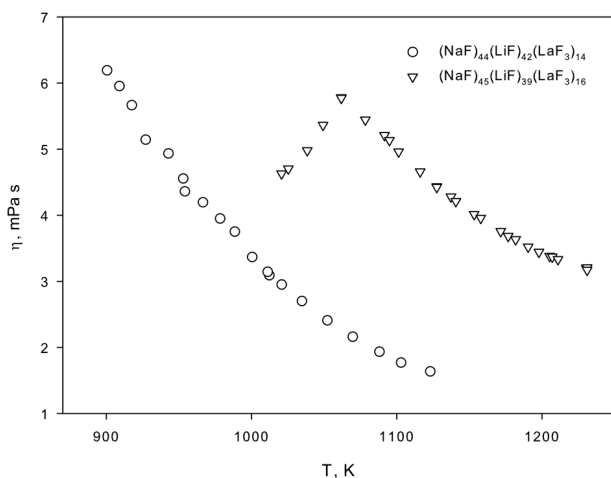


Fig. 1. Temperature dependences of the viscosity in NaF–LiF–LaF<sub>3</sub> melts [7]

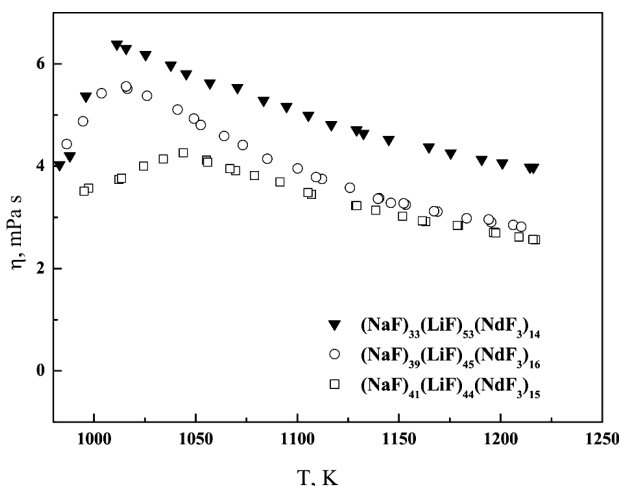


Fig. 2. Temperature dependences of the viscosity in NaF–LiF–NdF<sub>3</sub> melts [8]

were used. The cell design allowed the electric resistance and the thermal emf to be measured simultaneously. A high-temperature heater with three independently controllable heating elements made it possible to maintain a uniform temperature field within a working interval with an error of 0.2–0.3 K while measuring the electric resistance or to create a temperature drop of 15–20 K along the cell while measuring the thermoelectric power. The components were weighted with an accuracy of  $10^{-4}$  g, synthesized in quartz ampoules, which were pumped out to a residual pressure of 10–15 Pa, soldered, and poured immediately into cells. The experimental installation and

the measurement procedure were described in work [6]. The determination error did not exceed 2% for the conductivity  $\sigma(T)$  and 5% for the thermal emf  $S(T)$ .

### 3. Experimental Results and Their Discussion

In Figs. 1 and 2, the results obtained for the temperature dependence of the viscosity in ionic fluid systems are depicted. As one can see from Fig. 1, for specimen E(La)—this is the NaF–LiF–LaF<sub>3</sub> system with the eutectic composition—the viscosity decreases as the temperature grows within the whole studied interval. The processing of obtained experimental data with the help of the Arrhenius law

$$\eta(T) = \eta_0 \exp\left(\frac{Q}{RT}\right), \quad (1)$$

where  $\eta_0$  is a constant, and  $Q$  the activation energy of a viscous flow, gave the following values:  $Q = 55 \pm 3$  kJ/mol in a temperature interval of 900–970 K and  $Q = 36 \pm 3$  kJ/mol in a temperature interval of 970–1150 K.

Figure 2 also demonstrates the temperature dependence of the viscosity in the ionic liquid system NaF–LiF–LaF<sub>3</sub>, but with the peritectic composition, specimen P(La). As one can see, as the temperature decreases from the maximum, the viscosity of specimen P(La) grows and reaches a maximum value at the temperature  $T = 1080 \pm 5$  K. If the temperature decreases below 1080 K, the viscosity decreases. The same behavior is demonstrated by the temperature dependences of the viscosity for specimens E(Nd), P<sub>1</sub>(Nd), and P<sub>2</sub>(Nd) of the system NaF–LiF–NdF<sub>3</sub>. The viscosity maximum (see Fig. 2) was obtained at a temperature of  $1005 \pm 5$  K for eutectic specimen E(Nd) and at temperatures of  $1010 \pm 5$  K and  $1045 \pm 5$  K for specimens P<sub>1</sub>(Nd) and P<sub>2</sub>(Nd), respectively. It should be noted that the differences between the viscosity maximum temperature and the melting temperature are identical for all specimens within the measurement error. The existence of such special points located by 150–160 K above the melting temperatures can be explained by the fact that, in the examined temperature interval, the melts NaF–LiF–LaF<sub>3</sub> and NaF–LiF–NdF<sub>3</sub> are in the nonequilibrium state as a result of the incongruent melting of NaLaF<sub>4</sub>, NaNdF<sub>4</sub>, and Na<sub>5</sub>Nd<sub>9</sub>F<sub>32</sub> compounds. It is the inhomogeneity of a liquid system

that gives rise to the inapplicability of the Shvidkovskii formulas [9] used for the calculation of the viscosity. Therefore, the Shvidkovskii method does not allow one to determine the viscosity for specimen P(La) below  $1080 \pm 5$  K, for specimen E(Nd) below  $1005 \pm 5$  K, for specimen P<sub>1</sub>(Nd) below  $1010 \pm 5$  K, and for specimen P<sub>2</sub>(Nd) below  $1045 \pm 5$  K. At the same time, it should be noted that measurements of this kind make it possible to determine the maximum temperatures, at which the NaLaF<sub>4</sub> compound has not been incongruently melted yet in the NaF–LiF–LaF<sub>3</sub> system, and the NaNdF<sub>4</sub> and Na<sub>5</sub>Nd<sub>9</sub>F<sub>32</sub> compounds in the NaF–LiF–NdF<sub>3</sub> one. The analysis of Figs. 1 and 2 shows that the changes in the melt composition substantially affect the viscosity of an ionic fluid system. For instance, the eutectic–peritectic transition in the system with La in a temperature interval from 1050 to 1250 K makes the viscosity of the liquid NaF–LiF–LaF<sub>3</sub> system twice as high. The same transition in the NaF–LiF–NdF<sub>3</sub> melt reduces its viscosity by a factor of 1.5.

In Figs. 3 and 4, the measurement results for the temperature dependences of the thermal emf in NaF–LiF–LaF<sub>3</sub> and NaF–LiF–NdF<sub>3</sub> melts are presented. As one can see from Fig. 3, the interval of thermoelectric power variation in the NaF–LiF–LaF<sub>3</sub> system is twice as narrow for the peritectic composition in comparison with that for the eutectic one. For the NaF–LiF–NdF<sub>3</sub> system, the intervals of  $S$  variation for the eutectic and peritectic compositions practically coincide. Attention is attracted by the fact that, in the La-containing systems, the measured dependence  $S(T)$  changes, as the temperature grows, from negative values at the melting point, whereas  $S(T)$  is positive at the melting point for the system with Nd. For growing temperatures,  $S(T)$  increases in both systems; however,  $S(T)$  reaches positive values for specimens with lanthanum and remains negative for specimens with neodymium. As is seen from Fig. 2, *a*, there are minima in the dependences  $S(T)$  for E(La) and P(La) specimens at  $950 \pm 5$  K and  $1040 \pm 5$  K, respectively. In the dependence  $S(T)$  for specimens with neodymium, there are also minima (see Fig. 2) at temperatures  $970 \pm 5$  K for E(Nd),  $990 \pm 5$  K for P<sub>1</sub>(Nd), and  $1040 \pm 5$  K for P<sub>2</sub>(Nd) specimens, at which the derivative changes its sign.

By comparing Figs. 3 and 4, we may emphasize that the temperature dependence  $S(T)$  for the NaF–LiF–NdF<sub>3</sub> system can be approximately described

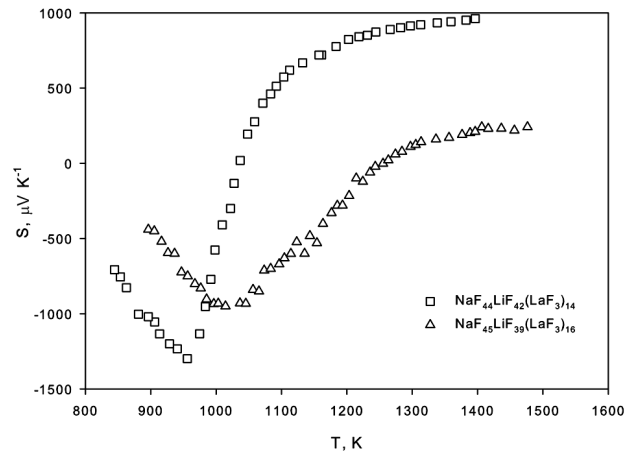


Fig. 3. Temperature dependences of the thermoelectric power in NaF–LiF–LaF<sub>3</sub> melts [7]

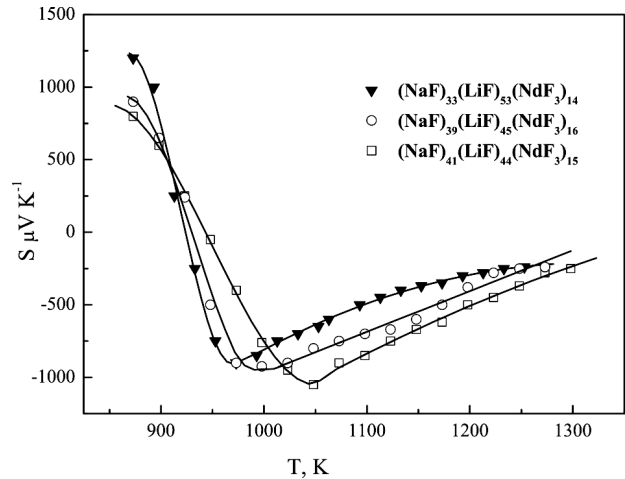


Fig. 4. Temperature dependences of the thermoelectric power in NaF–LiF–NdF<sub>3</sub> melts [8]

with the use of two  $\frac{dS}{dT}$  derivatives with opposite signs. At the same time, a similar description of  $S(T)$  in the NaF–LiF–LaF<sub>3</sub> system requires three  $\frac{dS}{dT}$  derivatives. One of the reasons that are responsible for such a behavior of the temperature dependence of the thermal emf and its relatively high absolute values (about  $1000 \mu\text{V/K}$ ) in comparison with those in liquid metals (about  $10 \mu\text{V/K}$ ) and liquid semiconductors (about  $100 \mu\text{V/K}$ ) is the heat transfer by ions, which makes a substantial contribution to  $S(T)$ , the latter being probably sensitive to the structure of salt melts [10, 11]. Note that, in the liquid state, the researched specimens of both systems consist of oppositely charged ions and a small fraction of non-

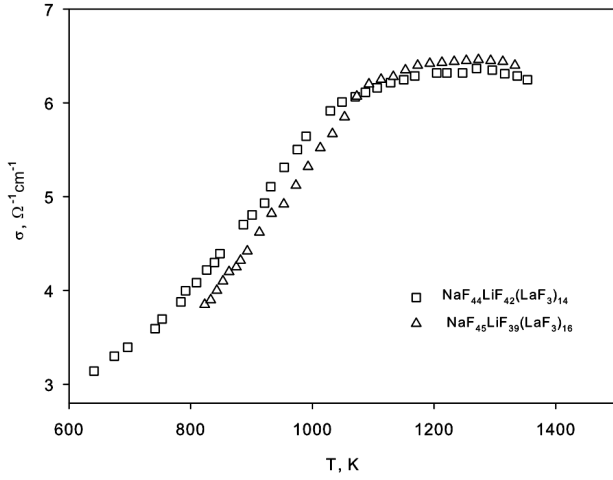


Fig. 5. Temperature dependences of the conductivity in NaF–LiF–LaF<sub>3</sub> melts [7]

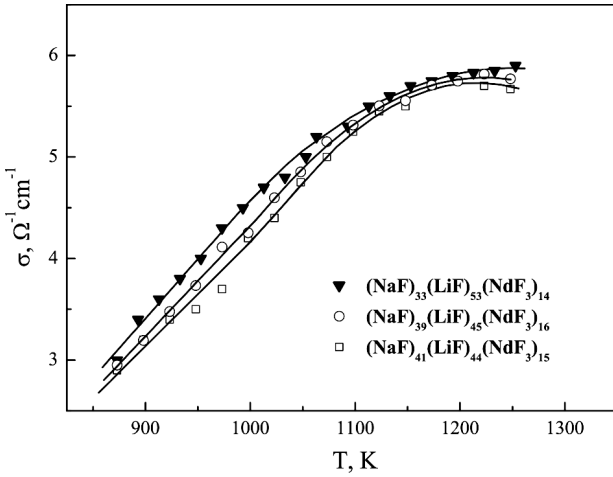


Fig. 6. Temperature dependences of the conductivity in NaF–LiF–NdF<sub>3</sub> melts [8]

dissociated molecules. Therefore, the melt structure depends both on the initial composition of components and their interaction, on the one hand, and on the temperature, on the other hand. The behavior of the thermal emf in such ionic liquid systems can be analyzed on the basis of the equation

$$S(T) = \frac{1}{T} \left( \sum \frac{Q_i^+}{e_0 z_i} t_i^+ - \sum \frac{Q_i^-}{e_0 z_i} t_i^- - \frac{Q_e}{e_0} t_e \right) - A, \quad (2)$$

where  $e_0$  is the electron charge;  $Q_i^+$ ,  $Q_i^-$ , and  $Q_e$  are the transfer heats for the  $i$ -th positive ion,  $i$ -th negative ion, and electron, respectively;  $t_i^+$ ,  $t_i^-$ , and  $t_e$  are

the partial contributions of the  $i$ -th positive ion,  $i$ -th negative ion, and electron, respectively, to the transferred charge; and  $A$  is a constant for the given ionic fluid system. The change in the sign of the derivative  $\frac{dS}{dT}$  is connected with a change of the dominating contribution to the thermal emf made by ions of either sign.

From formula (2), we get the temperature, at which  $S(T) = 0$ :

$$T_{S=0} = \frac{1}{A} \left( \sum \frac{Q_i^+}{e_0 z_i} t_i^+ - \sum \frac{Q_i^-}{e_0 z_i} t_i^- - \frac{Q_e}{e_0} t_e \right). \quad (3)$$

This value is governed by the transfer heats of ions and electrons, as well as by the partial contributions of those particles to the total transferred charge. As is seen from Eq. (3), there is only one temperature, at which the curve  $S(T)$  intersects the straight line  $S = 0$ , which is confirmed by the experiment.

It should be noted that, for specimens with lanthanum, the temperature dependence  $S(T)$ , besides the minimum, has another special point, at which the derivative  $\frac{dS}{dT}$  drastically changes its value. This point is observed at the temperature  $T = 1100 \pm 10$  K for eutectic specimens and  $T = 1300 \pm 10$  K for peritectic ones. In our opinion, the drastic change of the derivative at the indicated temperatures is induced by the third term in formula (3), which is characteristic of the studied systems with lanthanum, but is absent in the systems with neodymium. Attention is attracted by the fact that those points in the  $S(T)$  curves testify to qualitative modifications in the NaF–LiF–LaF<sub>3</sub> melt structure, which correlates with the disappearance of the front peak in the structural factor.

In Figs. 5 and 6, the temperature dependences of the dc electric conductivity in the NaF–LiF–LaF<sub>3</sub> and NaF–LiF–NdF<sub>3</sub> melts are exhibited. In general, the researched melts with lanthanum and neodymium, both eutectic and peritectic, behave themselves as semiconductors: as the temperature increases, their conductivity grows following the law

$$\sigma = \sigma_0 \exp[-\Delta E/2kT], \quad (4)$$

where  $\Delta E$  is the conductivity activation energy. A more detailed analysis of Fig. 5 shows that, in the case of lanthanum-containing systems, such a semiconductive dependence of the conductivity on the temperature is obeyed up to a temperature of 1100 K for spec-

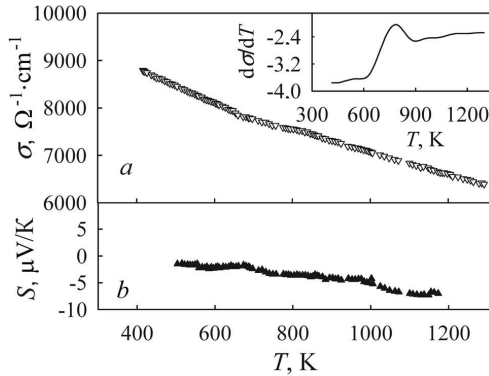


**Fig. 7.** Temperature dependence of the conductivity  $\sigma$  and its derivative (the inset) (a) and the temperature dependence of the thermoelectric power  $S$  for the eutectic melt  $\text{Pb}_{44}\text{Bi}_{56}$  [15] (b)

imen E(La) and to a temperature of 1300 K for specimen P(La). At higher temperatures, the conductivity decreases, which is typical of liquid metals. The value of  $\Delta E$  found from Eq. (5) equals  $0.29 \pm 0.01$  eV for E(La) specimen and  $0.31 \pm 0.01$  eV for P(La) one. In Fig. 6, the temperature dependences  $\sigma(T)$  for specimens E(Nd),  $\text{P}_1(\text{Nd})$ , and  $\text{P}_2(\text{Nd})$  are shown. Unlike the specimens with lanthanum, no transition from the semiconductive conductivity to the metallic one is observed, and the determined values for the  $\Delta E$  quantity are:  $\Delta E = 0.42 \pm 0.01$  eV for E(Nd) specimen,  $\Delta E = 0.44 \pm 0.01$  eV for  $\text{P}_1(\text{Nd})$  specimen, and  $\Delta E = 0.32 \pm 0.01$  eV for  $\text{P}_2(\text{Nd})$  specimen.

The researches of the melts of eutectic binary and ternary metallic systems also revealed an ambiguous inconsistent behavior of their physical properties. The results obtained and their interpretation are based on the model of a statistical distribution of atoms in the melt, the quasieutectic model. Eutectic melts can be considered as an alternation of micro-sized regions with smeared boundaries, in which the atomic concentrations are close to those in solid eutectic solutions and between which there is a permanent mass transfer. Direct structural researches provide no unambiguous information concerning the micro-sized inhomogeneous structure of eutectic melts. A quantitative estimation of the results testifies that not only the quasieutectic or statistical distribution of atoms in the melts is possible, but also an intermediate one.

The measurements of  $\sigma(T)$ ,  $S(T)$ , and  $\eta(T)$  in eutectic systems did not reveal considerable modifi-

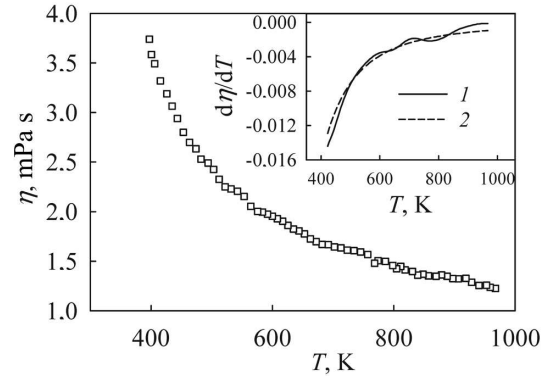


**Fig. 8.** Temperature dependence of the viscosity  $\eta$  and its derivative (the inset) for the eutectic melt  $\text{Pb}_{44}\text{Bi}_{56}$ : experiment (1) and theory (2) [15]

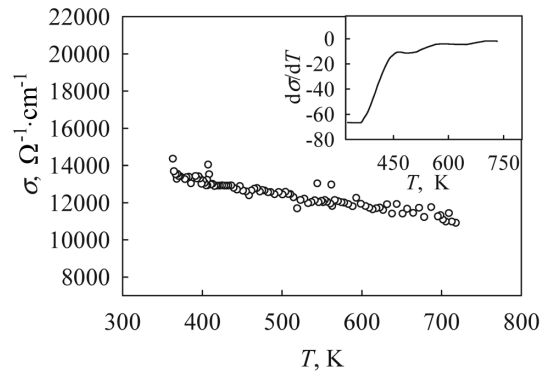


**Fig. 9.** Temperature dependence of the conductivity  $\sigma$  and its derivative (the inset) for the eutectic melt  $\text{Bi}_{43}\text{Sn}_{57}$  [15]

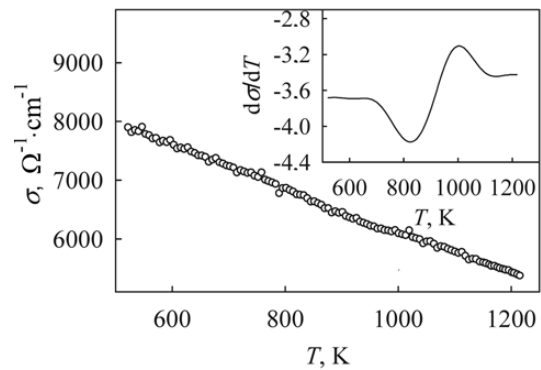


**Fig. 10.** Temperature dependence of the conductivity  $\sigma$  and its derivative (inset) for the eutectic melt  $\text{Pb}_{83}\text{Mg}_{17}$  [15]

cations in the indicated dependences. But their observed nonmonotonic character (Figs. 7–12) testifies that the melts undergo numerous structural transformations from the initial inhomogeneous liquid state,

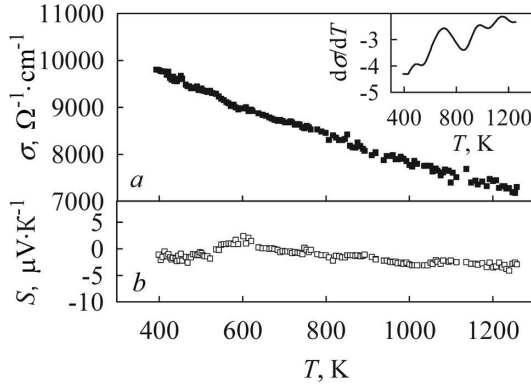


**Fig. 11.** Temperature dependence of the conductivity  $\sigma$  and its derivative (inset) (a) and temperature dependence of thermoelectric power  $S$  for the eutectic melt  $\text{Bi}_{46}\text{Pb}_{29}\text{Sn}_{25}$  [15] (b)

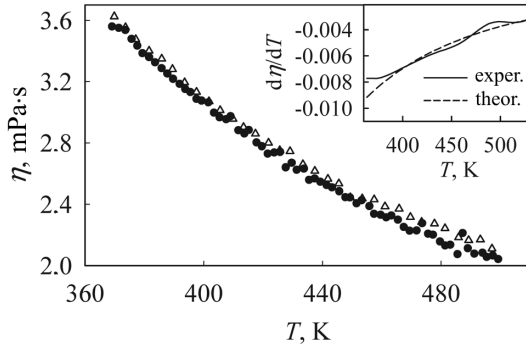


**Fig. 12.** Temperature dependence of the viscosity  $\eta$  and its derivative (inset) for the eutectic melt  $\text{Bi}_{46}\text{Pb}_{29}\text{Sn}_{25}$ : specimens 1 ( $\Delta$ ) and 2 ( $\bullet$ ) [15]

which emerges immediately after the melting, to the complete dissolution, which is gradually approached in the course of the subsequent heating [12–16]. At this structural reorganization, the previous bonds become destroyed, and new ones are formed. The quasieutectic structure itself can be regarded as a microemulsion or a microsuspension of dispersed nano- and microparticles enriched with one of the components and surrounded by a fused matrix of the other one. Owing to the difference between the densities of components, the sedimentation of aggregates takes place. However, the state of complete sedimentation is not reached, because of the intense Brownian motion resulting in a non-uniform distribution of particles over the altitude.

On the basis of Matthiessen’s rule, the dependence of physical properties on the ordering of components

can be used to explain the specific resistance of melts with a statistical distribution of impurity atoms,

$$\rho_{\text{st}} = \rho_0 + \Delta\rho, \quad (5)$$

where  $\rho_0$  is the matrix resistivity, and  $\Delta\rho$  an additional resistivity generated by impurities. The latter change the energy spectrum and the mean free path of charge carriers. Then, Eq. (5) can be rewritten in the form [16]

$$\rho_{\text{st}} = \frac{12\pi^3 \hbar}{S_{\text{F}}^{\text{st}} e^2 l_{\text{st}}}, \quad (6)$$

where  $S_{\text{F}}^{\text{st}} = 4\pi k^2$  is the Fermi surface area for free electrons,  $k = 2\pi(3N/4\pi)^{1/3}$ ,  $N$  is the atomic concentration, and  $l_{\text{st}}$  the electron mean free path.

The formation of microaggregates that include atoms of the same kind has a fluctuation character and cannot be accompanied by considerable changes in the energy spectrum of electrons in comparison with similar processes running in the statistical melt. However, the character of the charge carrier scattering has to change owing to a variation of the charge carrier mobility. If, according to the statistical distribution,  $\kappa$  is the fraction of scattering centers, and  $1 - \kappa$  is the fraction of atoms in microaggregates, the conductivity of a melt with a similar mixed distribution equals

$$\sigma = \frac{S_{\text{F}} e^2}{12\pi^3 \hbar} [\kappa l_{\text{st}} + (1 - \kappa) l_{\text{eut}}], \quad (7)$$

where  $l_{\text{eut}}$  is the mean free path of electrons in microaggregates.

At high temperatures, the thermoelectric power is mainly determined by its diffusion component and has the following expression for any metallic melt:

$$S = \frac{\pi^2 k^2 T}{3e} \left( \frac{d(\ln \sigma)}{dE} \right)_{E=E_{\text{F}}}. \quad (8)$$

Assuming that the wave vector at the Fermi level does not depend on the short-range order, the total thermal emf looks like

$$S = t \frac{\sigma^{\text{st}}}{\sigma} S^{\text{st}} + (1 - t) \frac{\sigma^{\text{eut}}}{\sigma} S^{\text{eut}}, \quad (9)$$

where

$$S^{\text{st}} = \frac{\pi^2 k^2 T}{3e} \left( \frac{d(\ln \sigma^{\text{st}})}{dE} \right)_{E=E_{\text{F}}} \quad (10)$$

is the thermal emf in a statistically ordered melt, and

$$S^{\text{eut}} = \frac{\pi^2 k^2 T}{3e} \left( \frac{d(\ln \sigma^{\text{eut}})}{dE} \right)_{E=E_F} \quad (11)$$

is the thermal emf under the eutectic ordering. Those two types of short-range ordering govern the behavior of physical properties of the solution.

The deviation of the concentration dependences of properties from the linearity, while approaching the eutectic composition, is a result of the formation of a micro-scaled inhomogeneous structure, which is associated with the presence of regions with different thermodynamic stabilities. These regions are separated, like those in monotectics, by spinodal and binodal lines. However, in the case concerned, there is no explicitly pronounced phase separation. Those regions are anomalous concentration fluctuations, which affect the modification of ordinary physical properties. This phenomenon can be regarded as a certain type of microsegregation. After the melting of the specimen, the quasieutectic structure of the heterogeneous melt survives, and the concentration gradient emerges along the specimen height. It is supposed that, in the temperature interval where the dependence  $\sigma(T)$  is linear (the slope  $d\sigma/dT$  is almost constant), reversible changes in both the melt composition and the particle size take place. The particles are in a metastable equilibrium with the matrix. After achieving a certain temperature, which is specific for every composition and manifests itself either as a bend in the  $\sigma(T)$  curve or as a drastic growing of  $d\sigma/dT$ , the dissolution of particles begins. Since the interfacial tension decelerates this process, the micro-sized inhomogeneous structure of a melt can survive even at rather high temperatures.

In work [17], by analyzing a melt of the eutectic Pb–Sn system, the limits of micro-sized inhomogeneous stability in the eutectic melts were estimated. The researches of temperature intervals with revealed anomalies in other similar systems showed that, in eutectic systems, the temperature maximum on the spinodal can considerably exceed  $2T_{\text{eut}}$ .

The behavior of examined properties testifies that the eutectic melt is heterogeneous at the microscopic level, being similar to the monotectic one [18–23]. However, the start of the crystallization in eutectics does not allow the tendency to the phase separation

in the liquid state to be clearly observed. Therefore, melts are macroscopically homogeneous at temperatures considerably above the critical one, and all available inhomogeneities can be described by Poisson concentration fluctuations with a short phase coherence length. In this case, the electron-ion interactions, which stabilize the system with respect to phase separation, and the electron-electron ones, which govern the screening of electrostatic forces in the system, play equally important roles. If the temperature decreases, this macroscopic homogeneity remains to exist for some time, but, when approaching the critical region, the volume fraction of microinhomogeneities with different component concentrations starts to grow. Interactions between identical particles start to prevail. The reaction of the electronic subsystem to the temperature variation is faster than the reaction of the ionic one, which manifests itself in the concentration dependence of the screening radius. The emerged spatial inhomogeneity of the electron gas makes the system unstable and favors the development of concentration fluctuations in a vicinity of the critical region. As a consequence, there appear microscopic clusters, which grow as the demixing temperature is approached.

In the eutectic systems, which were analyzed here as a special case of systems with limited solubility of components, the dimensions of clusters belonging to one of the phases, although changing with the temperature, do not reach such values as in monotectic systems. In other words, they preserve their sedimentation stability up to the liquidus temperature.

#### 4. Conclusions

The temperature dependences of the viscosity, conductivity, and thermoelectric power in the ternary ionic fluid systems NaF–LiF–LaF<sub>3</sub> and NaF–LiF–NdF<sub>3</sub> and the ternary metallic melts of the systems Pb–Bi, Pb–Mg, Bi–Sn, and Bi–Pb–Sn with the eutectic compositions have been studied in a wide temperature interval, including the melting point. The physical properties of analyzed ionic fluid systems and metallic melts are compared. Ion-ion and electron-ion interactions are shown to play a substantial role in salt melts. In metallic melts, besides the electron-ion interaction, an important role belongs to the electron-electron one as well.

*The work was supported by the Ministry of Education and Science of Ukraine and the State Fund for Fundamental Researches.*

1. L.A. Bulavin, V.I. Lysov, and S.L. Revo, *Physics of Ion-Electronic Fluids* (Kyiv Univ., Kyiv, 2008) (in Ukrainian).
2. I.I. Adamenko and L.A. Bulavin, *Physics of Fluids and Liquid Systems* (ASMI, Kyiv, 2006) (in Ukrainian).
3. N.A. Azarenkov, L.A. Bulavin, and I.I. Zalyubovskii, *Nuclear Power Engineering* (Kharkiv Univ., Kharkiv, 2012) (in Russian).
4. L.A. Bulavin and V.K. Tartakovskiy, *Nuclear Physics* (Znannya, Kyiv, 2006) (in Ukrainian).
5. S. Mudry, V. Sklyarchuk, and A. Yakymovych, *J. Phys. Studies* **12**, 1601 (2008).
6. Yu. Plevachuk and V. Sklyarchuk, *Meas. Sci. Technol.* **12**, 23 (2001).
7. L.A. Bulavin, Yu.O. Plevachuk, V.M. Sklyarchuk, A.O. Omelchuk, N.V. Faidiuk, and G.M. Savchuk, *Yadern. Fiz. Energ.* **14**, 154 (2013).
8. L. Bulavin, Yu. Plevachuk, V. Sklyarchuk, A. Omelchuk, N. Faidiuk, R. Savchuk, I. Shtablavyi, and V. Vus, *Nucl. Eng. Des.* **270**, 60 (2014).
9. E.G. Shvidkovskii, *Some Problems in the Viscosity of Molten Metals* (Gostekhizdat, Moscow, 1955) (in Russian).
10. L.A. Bulavin, A.O. Omelchuk, N.V. Faidiuk, V.M. Sklyarchuk, Yu.O. Plevachuk, V.S. Kopan, and R.N. Savchuk, *Ukr. J. Phys.* **59**, 769 (2014).
11. L. Bulavin, Y. Plevachuk, V. Sklyarchuk, I. Shtablavyi, N. Faidiuk, and R. Savchuk, *J. Nucl. Mater.* **433**, 329 (2013).
12. I. Kaban, W. Hoyer, Yu. Plevachuk, and V. Sklyarchuk, *J. Phys.: Condens. Matter*, **16**, 6335 (2004).
13. Yu. Plevachuk, V. Sklyarchuk, S. Eckert, and G. Gerbeth, *J. Nucl. Mater.* **373**, 335 (2008).
14. Yu. Plevachuk, V. Sklyarchuk, G. Gerbeth, and S. Eckert, *Int. J. Mater. Res.* **101**, 839 (2010).
15. Yu. Plevachuk, V. Sklyarchuk, A. Yakymovych, and G. Gerbeth, *J. Non-Cryst. Solids* **354**, 4443 (2008).
16. Yu. Plevachuk, V. Sklyarchuk, A. Yakymovych, B. Willers, and S. Eckert, *J. Alloy Compd.* **394**, 63 (2005).
17. V. Sklyarchuk, A. Yakymovych, I. Shtablavyi, I. Sheverno-ga, M. Kozlovs'kyi, R. Hairulin, and S. Stankus, *Ukr. Fiz. Zh.* **55**, 980 (2010).
18. B. Sokolovskii, Yu. Plevachuk, and V. Didoukh, *Phys. Status Solidi A* **148**, 123 (1995).
19. V. Didoukh, Yu. Plevachuk, and B. Sokolovskii, *J. Phase Equilib.* **17**, 414 (1996).
20. H. Neumann, Yu. Plevachuk, and F. Allenstein, *Mater. Sci. Eng. A* **361**, 155 (2003).
21. Yu. Plevachuk, V. Sklyarchuk, O. Alekhin, and L. Bulavin, *J. Mol. Liq.* **127**, 33 (2006).
22. Yu.O. Plevachuk, V.M. Sklyarchuk, O.D. Alekhin, and L.A. Bulavin, *J. Phys. Studies* **9**, 333 (2005).
23. Yu. Plevachuk, V. Sklyarchuk, O. Alekhin, O. Bilous, and L. Bulavin, *J. Non-Cryst. Solids* **353**, 3310 (2007).

Received 08.06.15.

Translated from Ukrainian by O.I. Voitenko

*В.М. Склярчук, Ю.О. Плевачук,  
А.О. Омелчук, Н.В. Файдюк*

**В'ЯЗКІСТЬ, ЕЛЕКТРОПРОВІДНІСТЬ,  
ТЕРМО-ЕРС ІОННИХ ТА ІОННО-ЕЛЕКТРОННИХ  
РІДИННИХ СИСТЕМ ЕВТЕКТИЧНОГО СКЛАДУ**

**Резюме**

Досліджено та порівняно температурні залежності в'язкості, електропровідності та термо-ерс іонних та іонно-електронних рідинних систем евтектичного складу в широкому температурному інтервалі, що включає температури плавлення досліджених сплавів.